jove

Laser Ablation and Intravital Microscopy to Study Intestinal Remodeling

Dimitrios Laskaris[*,1,2], **Maria Azkanaz**[*,1,2], **Mijke A. de Vreij-Kruidenier**[3], **Doreen van Rijswoud-Ram**[3], **Hendrik A. Messal**[1,2], **Jacco van Rheenen**[1,2]

[1] Department of Molecular Pathology, The Netherlands Cancer Institute [2] Oncode Institute [3] Animal Laboratory Facility, The Netherlands Cancer Institute

[*] These authors contributed equally

Corresponding Authors

Hendrik A. Messal
h.messal@nki.nl

Jacco van Rheenen
j.v.rheenen@nki.nl

Citation

Laskaris, D., Azkanaz, M., de Vreij-Kruidenier, M.A., van Rijswoud-Ram, D., Messal, H.A., van Rheenen, J. Laser Ablation and Intravital Microscopy to Study Intestinal Remodeling. *J. Vis. Exp.* (196), e64756, doi:10.3791/64756 (2023).

Date Published

June 9, 2023

DOI

10.3791/64756

URL

jove.com/video/64756

Abstract

Investigating intestinal recovery *in vivo* is an exquisite technical challenge. A lack of longitudinal imaging protocols has prevented deeper insights into the cell and tissue scale dynamics that orchestrate intestinal regeneration. Here, we describe an intravital microscopy method that locally induces tissue damage at the single crypt scale and follows the regenerative response of the intestinal epithelium in living mice. Single crypts or larger intestinal fields were ablated by a high-intensity multiphoton infrared laser in a time- and space-controlled manner. Subsequent long-term repetitive intravital imaging enabled the tracking of the damaged areas over time and allowed for the monitoring of crypt dynamics during tissue recovery over a period of multiple weeks. Crypt remodeling events such as crypt fission, fusion, and disappearance were observed in the neighboring tissue upon laser-induced damage. This protocol enables the study of crypt dynamics both in homeostatic and pathophysiological settings, such as aging and tumor initiation.

Introduction

The epithelial lining of the intestine is constantly challenged by gastric acids, toxins, and microbiota that can cause disruption of the epithelial barrier. Intestinal structure and tissue organization are specialized to constantly self-renew and repair damages. The single-layered epithelium of the small intestine is organized into crypt-villus units[1]. In homeostasis, self-renewing Lgr5^{+} intestinal stem cells that reside at the base of the crypt give rise to differentiated progeny. The differentiated daughter cells travel to the tip of the villus axis in a conveyer belt fashion, where they are shed so that the intestinal lining is replenished in 3-5 days[2,3].In the long term, not all Lgr5^{+} cells contribute equally to tissue renewal, as

this also depends on the ability of cells to move against the conveyer belt toward the base of the crypt (i.e., retrograde movement)[4,5]. Indeed, upon ablation of Lgr5$^+$ cells by, for example, radiation, progenitor cells outside of the base of the crypt move into the base to dedifferentiate and replenish the stem cell pool[6,7,8].

Acute inflammation can cause the loss of Lgr5$^+$ stem cells[9,10]. In addition to stem cell loss, many external factors can cause acute damage to the epithelium at the crypt scale. Radiation, chemical treatments, and antibiotics have been shown to injure intestinal crypts and villi[11]. Larger fields of crypts and villi can be affected by bacterial, viral, and parasitic infections[12]. The intestine possesses a remarkable ability to recover from internal and external damage at the crypt scale by crypt fission (a division of one crypt into two)[13]. Upon wounding, crypts in the area adjacent to the damage undergo fission to replenish the crypt numbers. This phenomenon also occurs, although to a lesser extent, during homeostasis[14,15]. To counterbalance a potential increase in crypt numbers during homeostasis, crypts can also fuse (merging two crypts into one)[16,17]. Whether crypt fusion also plays a role in reestablishing crypt numbers after wounding is unknown. Moreover, the dynamics and regulatory factors of this process remain to be elucidated.

Injury models are indispensable to study tissue regeneration *in vivo*. Various injury models have been utilized to study intestinal tissue regeneration. Previous experimental strategies employed high-dose radiation to deplete stem cell pools[18] or treatment with dextran sulfate sodium (DSS) to induce chronic and acute colitis and crypt loss in mice[19,20]. Single-cell ablation by genetic or optic means has been used to refine tissue damage and considered an attractive tool to disentangle the role of stem and progenitor cells[21,22] and study vascular regeneration[23]. Additionally, a biopsy-injury system has been developed to induce damage in larger fields of several crypts and villi[24]. Importantly, the response to the damaging insult may vary along the proximal-distal axis of the intestine, as reported for radiation, which caused more damage in the small intestine than in the colon[25]. This highlights the need for targeted methods that control both the extent of the damaging insult and its localization in the intestinal tract.

Damage extent and recovery have conventionally been assessed by static means, which provide limited information about the dynamics of tissue recovery. Intravital microscopy (IVM) has opened unique opportunities to quantify stem cell behavior, epithelial remodeling, and regeneration in many organs[26,27,28,29,30], and has provided impactful insights into intestinal biology[4,5,21,31,32,33,34,35,36].

Here, we describe a method to cause spatiotemporal-defined intestinal damage and capture the recovery of the intestinal epithelial lining. We utilize two photon-based laser ablation to damage intestinal crypts and follow the immediate wound response and long-term recovery by repetitive intravital microscopy. Our protocol allows one to map the regenerative remodeling of the intestinal tissue architecture in response to local tissue damage. Crypt dynamics, including fission and fusion events, can be readily quantified and tracked over time. The application of laser ablation and repetitive intravital imaging can be utilized as a platform to investigate the tissue-scale dynamics of intestinal architecture during homeostasis and pathophysiology, such as tumor initiation.

Protocol

All animal experiments described in this study were carried out in accordance with the guidelines and approval of the

Animal Welfare Body (AWB) of the Netherlands Cancer Institute (NKI).

NOTE: Consult the animal ethics committee of the institute before performing any animal experiments.

1. Preparation for surgery and intravital imaging

1. Pre-surgical treatments
    1. Induce 8-12-week-old K19-CreERT2[37]: Rosa26-mTmG[38] and Lgr5eGFP-IRES-CreERT2[18]: Rosa26-Confetti[39] mice by injecting tamoxifen dissolved in sunflower oil intraperitoneally 4-6 weeks prior to surgery (**Figure 1**).
    2. Apply analgesia. Inject 200 µL of buprenorphine (0.1 mg/kg body weight) diluted in NaCl 0.9% per 30 g mouse subcutaneously 30 min before surgery. Administer carprofen (0.067 mg/mL) in a bottle containing 125 mL of non-acidified autoclaved drinking water 24 h before surgery. Alternatively, administer a carprofen injection subcutaneously (5 mg/kg) 30 min before the start of surgery.
2. Preparation for surgery
    1. Introduce autoclaved sterile surgical tools in the biohazard cabinet.
    2. Turn on the heating pad and set the temperature to 37 °C.
3. Preparation for intravital imaging
    1. Turn on the temperature-controlled chamber of the microscope at least 4 h before imaging to allow sufficient time for temperature stabilization.
    NOTE: The time needed can vary depending on the machine used.
    2. Keep the temperature inside the climate chamber stable at 37 °C.
    3. Turn on the two-photon microscope, scanner, and laser.
    4. Launch the imaging software.
    5. Tune the wavelength of the laser to 960 nm and open the shutter.

2. Surgery and intravital imaging

1. Surgical exposure of the intestine
    1. Anesthetize the mouse using 2%-3% isoflurane and place it on a heating pad, covered with a sterile cloth. Check the depth of anesthesia by assessing the frequency and quality of breathing (one breath/second) and by checking the reflex of the mouse.
    2. Cover the eyes of the mouse with eye ointment.
    3. Inject 200 µL of pre-warmed sterile saline subcutaneously.
    4. Shave the abdomen and remove the hair. Change the sterile cloth in the surgical area.
    5. Insert a rectal probe to monitor the temperature of the mouse.
    NOTE: The temperature should be approximately 37 °C.
    6. Put on a new pair of sterile gloves.
    7. Clean the surgical area in a circular way with alternating scrubs of antiseptic solution followed by 80% ethanol three times. Remove excess ethanol with a sterile cotton swab.
    NOTE: It is critical to monitor the mouse for hypothermia at this point.

8. Cover the mouse with a sterile surgical drape.
9. Check the reflex of the mouse.
10. Make a ~10 mm vertical midline incision through the skin using a sterile scalpel.
11. Incise the linea alba using scissors to separate the rectus abdominis muscles and open the abdomen.
12. Find the cecum of the mouse using sterile cotton swabs drenched in sterile pre-warmed saline to use it as a reference point.
13. Make a small cut in a piece of sterile gauze, wet it in preheated sterile saline, and place it above the incision.
14. Take out the intestine with sterile cotton swabs drenched in pre-warmed sterile saline. Keep the intestine hydrated by adding sterile pre-warmed saline.
15. Place a sterile custom-made imaging chamber next to the mouse.
16. Transfer the mouse to the preheated sterile imaging box.
17. Place the intestine on the sterile glass of the imaging box. Place the head of the mouse inside the inhalation tube of the imaging box, as shown in **Figure 1**.
18. If necessary, secure the mouse with sterile flexible film and tape.
19. Place the imaging box containing the mouse in the microscope chamber.

2. Intravital imaging
    1. Monitor the mouse during imaging by checking the frequency and depth of breathing and temperature *via* a rectal probe every 15 min. The percentage of isoflurane should be kept between 1%-2%. Adjust if needed.
    2. Find a region in the intestine using the eyepiece of the microscope.
    3. Obtain a wide-field view of the region of interest using the microscope's internal camera, as seen in **Figure 2A**.
    4. Image the region of interest using the 960 nm laser of the multiphoton microscope. Adjust the laser power and wavelength according to the fluorophores used in the experiment.
    5. Acquire a 10-20 step z-stack of 3 µm of the region of interest.
3. Laser ablation
    1. Pick a single position or multiple positions from the tile imaged previously.
    2. Use the bleach point calibration function in the imaging software at a zoom of 32 and 124 x 124 pixel resolution with a scan speed 400 Hz, using the bidirectional scanning property for 3-10 s, depending on the size of damage aimed for. The initiation of damage in the crypt area can be recognized by an increase in autofluorescence in both the green and red channels.
    3. Repeat the previous two steps for multiple regions in the same mouse.
    4. After ablation, acquire z-stacks of the damaged regions to confirm the location and extent of the damage.
4. Closure of the surgical site

1. Place the mouse, while still under anesthesia, in a sterile suturing area.
2. Insert the exposed intestine back into the abdomen using sterile cotton swabs drenched in preheated sterile saline.
3. Suture the linea alba by performing a simple continuous suture using an absorbable 5-0 suture. Close the extremities of the suture with surgical knots.
4. Repeat the same step with the skin layer.
5. Switch off the isoflurane station and clean and sterilize the imaging box and inlay.
6. Clean the surgery tools with the surgical instrument cleaner, enzymatic cleaner, and surgical instrument lubricant. When dried, sterilize the surgery tools together with the surgery box in the autoclave.

5. Post-surgery care
    1. Let the mouse recover from surgery while the cage is placed on the heating pad for ~1 h.
    NOTE: Place the mouse with other cage mates if possible. Solitary housing is not necessary for recovery.
    2. Check the temperature of the mouse every 15 min during recovery.
    3. Inject 200 µL of buprenorphine (0.1 mg/kg body weight) diluted in NaCl 0.9% per 30 g mouse subcutaneously 6-12 h post-surgery.
    4. Administer carprofen (0.067 mg/mL) in a bottle containing 125 mL of non-acidified autoclaved drinking water for 72 h post-surgery.
    5. Weigh the mouse and monitor the welfare every day for 1 week post-surgery.

3. Repetitive surgery and intravital imaging

1. Surgery
    1. On the second time point (at least 1 week after the first imaging session), repeat steps 1.1.2, 1.2, 1.3, and 2.1.
2. Intravital imaging
    1. Repeat steps 2.2.1-2.2.3.
    2. Use the pattern of blood vessels to find the same regions of interest imaged on the first time point.
    3. Repeat steps 2.2.4 and 2.2.5.
3. Closure of the surgical site
    1. Repeat step 2.4.1.
    2. If the mouse is not meant to be imaged on another time point, sacrifice the mouse by performing cervical dislocation under terminal anesthesia. Otherwise, continue with the next step.
    NOTE: According to the guidelines of EU Directive 2010/63/EU, appendix IV, cervical dislocation is an acceptable method.
    3. Repeat steps 2.4.2-2.4.6.
4. Post-surgery care
    1. Repeat steps 2.5.1-2.5.5.

Representative Results

To demonstrate the type of results that can be obtained from the laser ablation method combined with intravital imaging, we performed an experiment as shown in **Figure 1**. First, we injected K19-CreERT2;mTmG (K19cre-mTmG)

and Lgr5eGFP-IRES-CreERT2;Rosa26-Confetti (Lgr5cre-Confetti) mice with tamoxifen to stochastically label cells with one of the Confetti colors (or green fluorescent protein [GFP] in the case of mTmG mice). K19-cre induces lineage tracing from all epithelial cells, while Lgr5-cre induces tracing from stem cells only[8,18,37]. The tamoxifen injection was administered 4-6 weeks before surgery and the first imaging session in order to obtain crypts in which all the cells are monoclonal for a certain color. Robust identification of the same tissue regions over several weeks is essential to track the fate of the same crypts over time. Inherent tissue architectural features, such as the vasculature, can be used as reliable tissue landmarks, and were here recorded with the internal camera of the microscope. In addition, labeling a small fraction of crypts with (at least two) different colors helped recognize the same crypts in each imaging session and following their behavior during the regenerative process after laser damage. Upon surgically exposing the intestine of the mouse and acquiring both camera and fluorescent images of the region of interest (**Figure 2A**), bleach point settings of the multiphoton laser can be used to ablate one or more crypts (**Figure 2B,C**). The initiation of damage could be recognized by an increase in autofluorescence in both the green and red channels. To study the dynamics of crypt recovery, the surgery and imaging procedure was repeated weeks/months after the first imaging session and tissue inherent structures (vasculature and patterns of clonally labelled crypts) were used as landmarks to find the exact same location of the injury (**Figure 2**). When this method was applied in Lgr5Cre-Confetti mice, where Lgr5-eGFP is expressed in a patchy manner, changes in crypt numbers and shapes following the laser-induced damage could be captured (**Figure 3**). While some regions showed no changes in the number and structure of crypts (**Figure 3B**), other regions showed extensive crypt remodeling, as seen in the number of crypt fission and fusion events (**Figure 3C**) and the loss of crypts 2 weeks after the laser-induced injury (**Figure 3D**). By introducing different sizes of damage and quantifying the fission, fusion, and disappearance events following ablation, as in the example shown in (**Figure 3E**), the dynamics of injury-induced regeneration can be mapped in different mouse models.

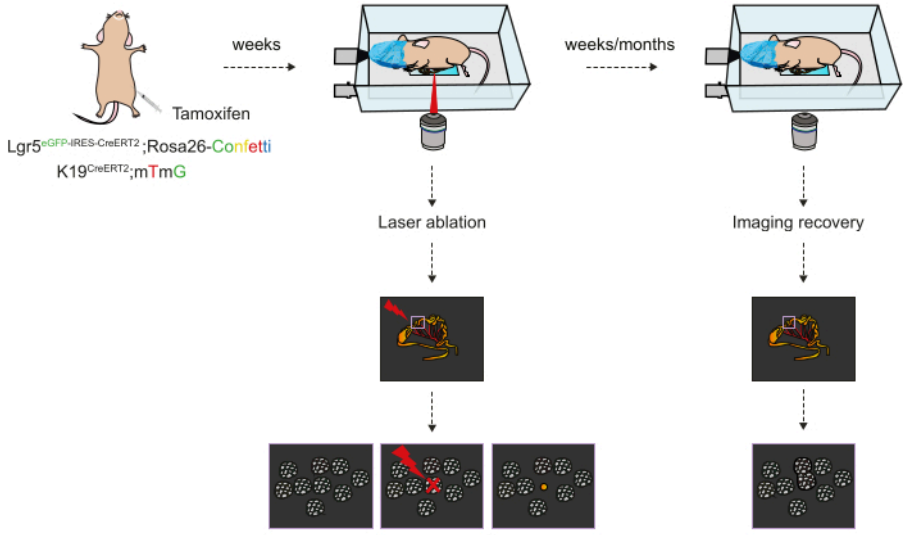

Figure 1: Schematic representation of the experimental setup. *In vivo* labeling of intestinal cells is achieved by injecting tamoxifen intraperitoneally in genetically modified mouse models to induce Cre-mediated recombination in intestinal crypts. After days or weeks (when the crypts are monoclonal for a certain color), the intestine is surgically exposed and subjected to laser ablation using a multiphoton microscope with a temperature-controlled chamber. The extent of crypt damage is characterized immediately after ablation and the mouse is allowed to recover from the procedure. Repeated surgical exposure and IVM are used to monitor intestinal recovery over time. The pattern and distribution of the blood vasculature and differently colored crypts are used to find back the same regions weeks or months after ablation. Crypt remodeling (e.g., fission or fusion) can be observed at the site of damage weeks after ablation. Please click here to view a larger version of this figure.

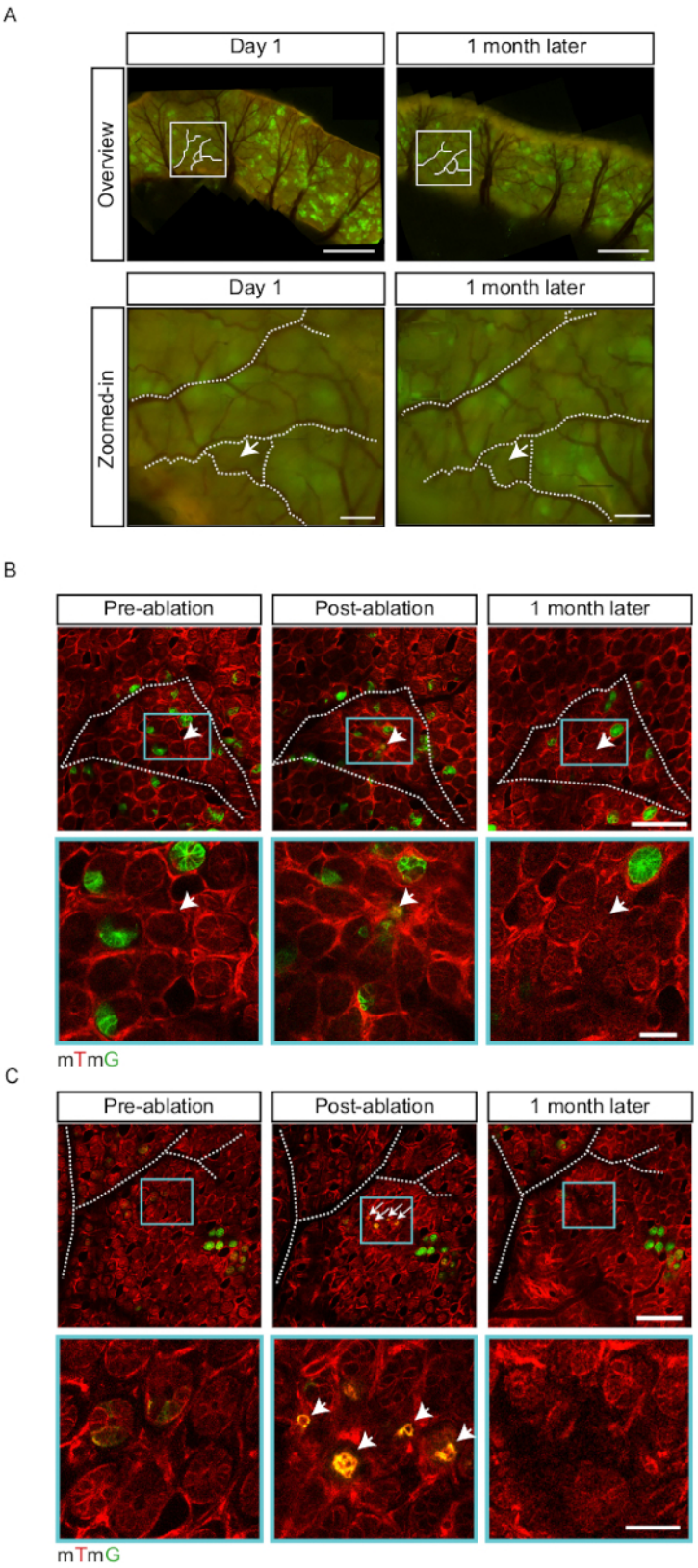

Figure 2: Longitudinal imaging of tissue regeneration upon laser-induced damage in the intestine. When the intestine is positioned in the exact same manner, blood vessels of the intestine can be used as a map to find and image the exact same regions. (**A**) Camera overview images of the intestine. Dashed white lines represent the pattern of the vasculature neighboring the site of damage (white box), used as a landmark to find the same laser-ablated region on another time point. The lower two images show the zoomed-in view of the white box. The arrow depicts the exact site of laser ablation at day 1 and 1 month later. (**B**) Fluorescent images of a single crypt damage captured by multiphoton microscope. The arrow in the blue box shows the site of the damage at day 1 and 1 month later. (**C**) Fluorescent images of a damaged field of crypts. The arrows in the blue box mark the region of the damage at day 1 and 1 month later. Scale bars: 1 mm (**A**, top); 0.25 mm (**A**, bottom); 200 µm (big overview **B** and **C**); and 50 µm (zoomed images **B** and **C**). Please click here to view a larger version of this figure.

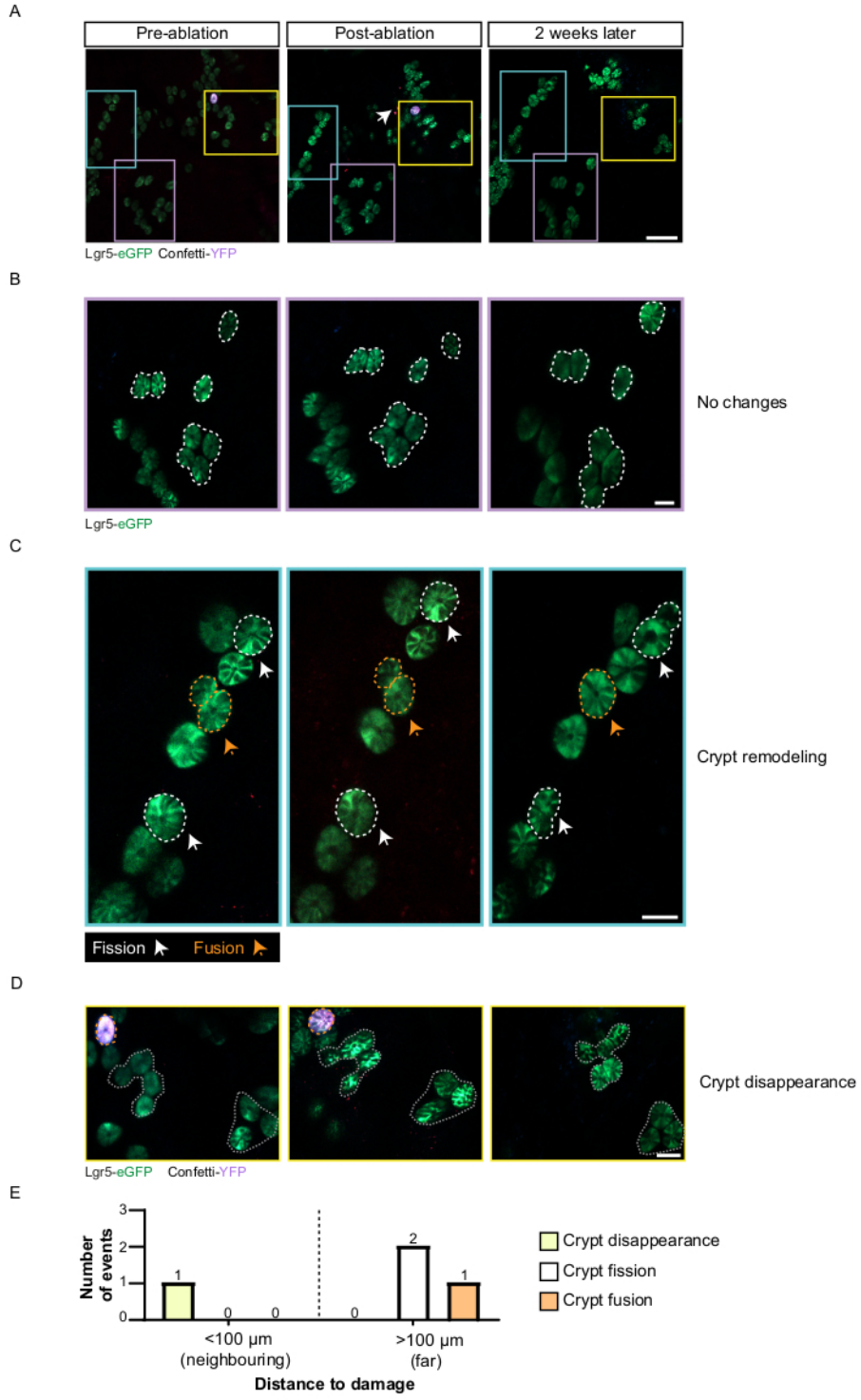

Figure 3: Intravital imaging of crypt fates following laser ablation. (**A**) Using the Confetti model, crypts labeled with different colors can be followed over time to map the dynamics of recovery. The white arrow depicts the site of laser ablation. The yellow box represents a neighboring region (<100 µm from the site of damage), while the blue and purple boxes

represent regions far (>100 µm) from the laser-ablated region. Different modes of regeneration are observed. (**B**) Some regions remain unchanged as in the purple box. (**C**) Other regions exhibit crypt remodeling in the form of crypt fission or fusion; the dashed white lines and arrows depict crypt fission events and the orange dashed lines and arrows depict crypt fusion events. (**D**) In some regions, crypt disappearance is observed, as in the yellow box where the crypt highlighted with an orange dashed line disappeared. (**E**) An example quantification showing the number of crypt remodeling events observed in the areas neighboring (i.e., less than 100 µm) and far from (i.e., more than 100 µm) the damage site. Scale bars: 200 µm (**A**); 50 µm (**B-D**). Please click here to view a larger version of this figure.

Discussion

This protocol combines microscopic laser ablation and longitudinal intravital microscopy to follow intestinal regeneration from early damage response to long-term tissue remodeling. The technique has been established in strict adherence to ethical considerations to induce and image microscopic laser ablation, and when followed precisely will maintain animal wellbeing. During surgery, it is important to make sure that the integrity of the intestine is well preserved. This can be achieved by gently handling the tissue with sterile wet cotton swabs, which prevents bleeding or drying out of the tissue. The extent of laser-induced microscopic damage should also be carefully assessed by imaging the different intestinal layers of the area after laser ablation. If the researcher wishes to adapt the frequency of the experimental steps described in this protocol, the animal ethics committee of the institute should be consulted before the experiment to establish the consequence on the welfare.

Repetitive intravital microscopy allows to monitor tissue recovery in the same mouse over time. Repeated surgical exposure of the intestine readily grants optical access to the entire intestinal tract. Tissue inherent features, such as the vasculature, serve as landmarks to identify the same intestinal regions in each imaging session. Thus, the same tissue region can be imaged over several weeks, which enables one to quantify long-term tissue regeneration in the same intestinal area in the same mouse. The spatiotemporal control offered by the combined surgery and imaging method brings the advantage that the same organ can be imaged under both homeostatic and regenerating conditions in the same mouse, which stands in contrast to previous whole-organ damage models where controls and regenerating samples originated from different mice[11,12,18,19,20]. Hence, our experimental setting minimizes the required number of animals needed for the experiment and reduces intra-animal variation.

Protocol troubleshooting should start with a review of the mouse and intestine handling technique, and a control of microscopy equipment and settings. There are many critical steps in this protocol that require extra attention. First, in order to ensure animal wellbeing and continuous high data quality, all work needs to be carried out in a clean sterile environment using aseptic technique, and mouse temperature should be maintained during surgery and each imaging session. Keeping the tissue hydrated with sterile, pre-warmed saline during imaging is essential and prevents tissue fibrosis.

To ensure that the experiment is carried out in a reproducible manner, it is important to align the lasers before use for optimal acquisition and to measure the power output of the multiphoton laser at the beginning of each session. Parameters such as the type of the objective, magnification, dwelling time, laser power, and wavelength have influences

on the extent of microscopic laser ablation and should be considered. In this study, both laser ablation and imaging are conducted with a laser power of 1.2 W (out of the lens) at a 960 nm wavelength through a Fluotar VISIR 25x/0.95 WATER objective. Changing the wavelength or optical scanning properties affects the extent of microscopic damage. A lower wavelength (such as 840 nm) translates into higher energy photons and often in a higher output of the laser, and may enhance microscopic damage. A higher zoom results in more energy per region, and therefore less time to ablate crypts, and vice versa. The pixel dwelling time can also be increased or decreased to change the speed of ablation and the extent of damage. When the imaged tissue is not stable (e.g., because of peristaltic movements), ablation needs to be performed rapidly. For this purpose, the speed of ablation should be optimized by, for example, increasing the zoom and/or laser output.

Finding the same intestinal region over multiple imaging sessions is another critical step that needs to be executed properly to ensure the success of the experiment. To do so, the intestine needs to be positioned in the exact same manner at all time points. We recommend to always use the cecum as a reference point to find the same regions in the small and large intestine. Gently stretching the tissue of interest with cotton swabs ensures that the region of interest is in range of the objective working distance and maximizes the number of regions that can be traced back. In addition, we recommend to always ablate and image multiple microscopic positions in each mouse to account for regions that may not be localized back in a later imaging session. If the regions cannot be found, even though the positioning of the intestine is correct, it can help to reposition the mouse and change the orientation of the exposed area. Tracking crypts over time can be cumbersome for experiments where larger intestinal fields of several adjacent crypts are ablated. Such damaging insults can evoke tissue remodeling beyond the epithelial monolayer, which can culminate in modification of the tissue landmarks used for tracking of the region over time. Choosing landmarks at a sufficient distance to the damaged site and capturing larger fields of view that surpass the damaged area by several hundred micrometers increases the chance for successful long-term experiments. In addition to incorrect positioning of the intestine on the microscope stage, peristaltic movements of the gastrointestinal tract may interfere with imaging. This problem may be ameliorated in two ways. If the frequency of movements is not too high, the process may be repeated in the same region with an increased exposure time. Alternatively, higher amounts of anesthesia can be used to decrease peristalsis. We recommend limiting higher doses of isoflurane to short adjustments. Altogether, the imaging sessions should be kept as short as possible, optimally below 3 h, to ensure fast recovery.

The combined laser ablation and longitudinal intravital microscopy approach has several advantages when compared with other damage models. Previous (chemical) damage models lacked the ability to locally confine the damaging insult[6,11,12,19,20]. Laser ablation overcomes this shortcoming by restricting the damage to a defined region of interest. This enables researchers to control the location of the injury, as well as the damage extent. Damage severity can be modulated to ablate crypts or entire microscopic intestinal fields to inform about regenerative responses at the crypt scale. In addition to spatial control, laser ablation also allows to precisely time the onset of damage, thereby surpassing the precision of previous drug, chemical, and infection models[9,10,11,12,19,20]. Our protocol expands on previous studies that used laser-induced thermal ablation as

a method to induce localized damage in the intestine[21,23]. Previous laser-induced damage models imaged local areas in the small intestine[21] or the luminal surface of the distal colon[23]. The combined surgery and laser ablation approach makes it possible to visualize the intestinal epithelium (crypts in particular) at a high resolution, and to perform laser ablation and follow-up imaging of tissue recovery in any position of the small intestine, cecum, and proximal colon. It captures the recovery of the same intestinal regions over time, allowing to visualize different layers of the intestine (mucosa, submucosa, muscularis, and serosa) as per the experimental setup. Our technique is mainly tailored for long-term repeated imaging for a period of multiple weeks/months. To study the short-term recovery dynamics of crypts (e.g., for several consecutive days following damage), the laser ablation approach described here can be combined with intravital imaging windows[27,28,40].

This protocol can be utilized for a multitude of research applications from diverse scientific areas that span regeneration, immunology, and cancer research. Longitudinal imaging of intestinal regeneration sheds light on the cellular dynamics that preserve epithelial integrity and barrier function, enable host defense against pathogens in the intestinal lumen, and that underlie the clearance and spread of oncogenic mutations. Each scientific question will cast unique demands on the extent of laser-induced damage and the duration of imaging. Fluorescent reporter mice and injected dyes can drastically expand and refine the data that can be acquired by allowing the visualization of any cell and structure of interest. For example, an Lgr5-CreERt2:Rosa26-Confetti mouse can be used to visualize stem cell progenies, whilst the Rosa26-mTmG reporter informs on tissue architecture. Together, these recent technological advances make intravital intestinal experimentation a lucrative tool to advance our understanding of intestinal biology and disease.

Disclosures

The authors have nothing to disclose.

Acknowledgments

This study was supported by the Netherlands Organization of Scientific Research NWO (Vici grant 09150182110004 to J.v.R. and Veni grant 09150161910151 to H.A.M), the OCENW.GROOT.2019.085 (to J.v.R), and an EMBO postdoctoral fellowship (grant ALTF 452-2019 to H.A.M).

References

1. Clevers, H. The intestinal crypt, a prototype stem cell compartment. *Cell.* **154** (2), 274-284 (2013).
2. Darwich, A. S., Aslam, U., Ashcroft, D. M., Rostami-Hodjegan, A. Meta-analysis of the turnover of intestinal epithelia in preclinical animal species and humans. *Drug Metabolism and Disposition.* **42** (12), 2016-2022 (2014).
3. Beumer, J., Clevers, H. Regulation and plasticity of intestinal stem cells during homeostasis and regeneration. *Development.* **143** (20), 3639-3649 (2016).
4. Ritsma, L. et al. Intestinal crypt homeostasis revealed at single-stem-cell level by in vivo live imaging. *Nature.* **507** (7492), 362-365 (2014).
5. Azkanaz, M. et al. Retrograde movements determine effective stem cell numbers in the intestine. *Nature.* **607** (7919), 548-554 (2022).
6. van Es, J. H. et al. Dll1^{+} secretory progenitor cells revert to stem cells upon crypt damage. *Nature Cell Biology.* **14** (10), 1099-1104 (2012).

7. Tomic, G. et al. Phospho-regulation of ATOH1 is required for plasticity of secretory progenitors and tissue regeneration. *Cell Stem Cell.* **23** (3), 436-443.e7 (2018).
8. Asfaha, S. et al. $Krt19^{+}/Lgr5^{-}$ cells are radioresistant cancer-initiating stem cells in the colon and intestine. *Cell Stem Cell.* **16** (6), 627-638 (2015).
9. Schmitt, M. et al. Paneth cells respond to inflammation and contribute to tissue regeneration by acquiring stem-like features through SCF/c-Kit signaling. *Cell Reports.* **24** (9), 2312-2328.e7 (2018).
10. Davidson, L. A. et al. Alteration of colonic stem cell gene signatures during the regenerative response to injury. *Biochimica et Biophysica Acta.* **1822** (10), 1600-1607 (2012).
11. Ijiri, K., Potten, C. S. Further studies on the response of intestinal crypt cells of different hierarchical status to eighteen different cytotoxic agents. *British Journal of Cancer.* **55** (2), 113-123 (1987).
12. Andersson-Rolf, A., Zilbauer, M., Koo, B. K., Clevers, H. Stem cells in repair of gastrointestinal epithelia. *Physiology.* **32** (4), 278-289 (2017).
13. Totafurno, J., Bjerknes, M., Cheng, H. The crypt cycle. Crypt and villus production in the adult intestinal epithelium. *Biophysical Journal.* **52** (2), 279-294 (1987).
14. Dekaney, C. M., Gulati, A. S., Garrison, A. P., Helmrath, M. A., Henning, S. J. Regeneration of intestinal stem/progenitor cells following doxorubicin treatment of mice. *American Journal of Physiology. Gastrointestinal and Liver Physiology.* **297** (3), G461-G470 (2009).
15. Cairnie, A. B., Millen, B. H. Fission of crypts in the small intestine of the irradiated mouse. *Cell and Tissue Kinetics.* **8** (2), 189-196 (1975).
16. Bruens, L., Ellenbroek, S. I. J., van Rheenen, J., Snippert, H. J. In vivo imaging reveals existence of crypt fission and fusion in adult mouse intestine. *Gastroenterology.* **153** (3), 674-677.e3 (2017).
17. Baker, A. M. et al. Crypt fusion as a homeostatic mechanism in the human colon. *Gut.* **68** (11), 1986-1993 (2019).
18. Barker, N. et al. Identification of stem cells in small intestine and colon by marker gene Lgr5. *Nature.* **449** (7165), 1003-1007 (2007).
19. Okayasu, I. et al. A novel method in the induction of reliable experimental acute and chronic ulcerative colitis in mice. *Gastroenterology.* **98** (3), 694-702 (1990).
20. Rakoff-Nahoum, S., Paglino, J., Eslami-Varzaneh, F., Edberg, S., Medzhitov, R. Recognition of commensal microflora by toll-like receptors is required for intestinal homeostasis. *Cell.* **118** (2), 229-241 (2004).
21. Choi, J. et al. Intestinal crypts recover rapidly from focal damage with coordinated motion of stem cells that is impaired by aging. *Scientific Reports.* **8** (1), 10989 (2018).
22. Tian, H. et al. A reserve stem cell population in small intestine renders Lgr5-positive cells dispensable. *Nature.* **478** (7368), 255-259 (2011).
23. Choi, M., Yun, S. H. In vivo femtosecond endosurgery: an intestinal epithelial regeneration-after-injury model. *Optics Express.* **21** (25), 30842-30848 (2013).
24. Seno, H. et al. Efficient colonic mucosal wound repair requires Trem2 signaling. *Proceedings of the National Academy of Sciences.* **106** (1), 256-261 (2009).

25. Hua, G. et al. Distinct levels of radioresistance in Lgr5$^+$ colonic epithelial stem cells versus Lgr5$^+$ small intestinal stem cells. *Cancer Research.* **77** (8), 2124-2133 (2017).
26. Rompolas, P. et al. Live imaging of stem cell and progeny behaviour in physiological hair-follicle regeneration. *Nature.* **487** (7408), 496-499 (2012).
27. Alieva, M., Ritsma, L., Giedt, R. J., Weissleder, R., van Rheenen, J. Imaging windows for long-term intravital imaging: General overview and technical insights. *Intravital.* **3** (2), e29917 (2014).
28. Rakhilin, N. et al. An intravital window to image the colon in real time. *Nature Communications.* **10** (1), 5647 (2019).
29. Messal, H. A. et al. Antigen retrieval and clearing for whole-organ immunofluorescence by FLASH. *Nature Protocols.* **16** (1), 239-262 (2021).
30. Farrelly, O. et al. Two-photon live imaging of single corneal stem cells reveals compartmentalized organization of the limbal niche. *Cell Stem Cell.* **28** (7), 1233-1247.e4 (2021).
31. Krndija, D. et al. Active cell migration is critical for steady-state epithelial turnover in the gut. *Science.* **365** (6454), 705-710 (2019).
32. Bruens, L. et al. Calorie restriction increases the number of competing stem cells and decreases mutation retention in the intestine. *Cell Reports.* **32** (3), 107937 (2020).
33. Bietar, B., Zhou, J., Lehmann, C. Utility of intestinal intravital microscopy for the study of CNS injury-induced immunodepression syndrome (CIDS). *Clinical Hemorheology and Microcirculation.* **79** (1), 137-147 (2021).
34. Erreni, M., Doni, A., Weigert, R. Method for acute intravital imaging of the large intestine in live mice. *Methods in Molecular Biology.* **2304**, 285-299 (2021).
35. Hiltensperger, M. et al. Skin and gut imprinted helper T cell subsets exhibit distinct functional phenotypes in central nervous system autoimmunity. *Nature Immunology.* **22** (7), 880-892 (2021).
36. Martínez-Sánchez, L. D. C. et al. Epithelial RAC1-dependent cytoskeleton dynamics controls cell mechanics, cell shedding and barrier integrity in intestinal inflammation. *Gut.* **72** (2), 275-294 (2022).
37. Means, A. L., Xu, Y., Zhao, A., Ray, K. C., Gu, G. A CK19(CreERT) knockin mouse line allows for conditional DNA recombination in epithelial cells in multiple endodermal organs. *Genesis.* **46** (6), 318-323 (2008).
38. Muzumdar, M. D., Tasic, B., Miyamichi, K., Li, L., Luo, L. A global double-fluorescent Cre reporter mouse. *Genesis.* **45** (9), 593-605 (2007).
39. Snippert, H. J. et al. Intestinal crypt homeostasis results from neutral competition between symmetrically dividing Lgr5 stem cells. *Cell.* **143** (1), 134-144 (2010).
40. Messal, H. A., van Rheenen, J., Scheele, C. L. An intravital microscopy toolbox to study mammary gland dynamics from cellular level to organ scale. *Journal of Mammary Gland Biology and Neoplasia.* **26** (1), 9-27 (2021).